JOURNAL OF GEOPHYSICAL RESEARCH, VOL. 111, C07026, doi:10.1029/2005JC003146, 2006

Click Here for Full Article

Surface drifter exchange between the North Atlantic subtropical and subpolar gyres

Elena Brambilla[1] and Lynne D. Talley[1]

Received 5 July 2005; revised 22 March 2006; accepted 25 April 2006; published 29 July 2006.

[1] Surface drifters deployed in the subtropical and subpolar North Atlantic from 1990 to 2002 show almost no connection between the subtropical and subpolar gyres; only one drifter crosses the intergyre boundary even though other data types (e.g., dynamic topography and tracers) suggest a major connection. Two of several possible causes for the lack of intergyre connectivity in this two-dimensional data set are examined: (1) undersampling and short drifter lifetime leading to underestimation of the northward flow, and (2) the southward mean Ekman velocity. Advection of a large number of long-lived synthetic drifters through the observed mean velocity results in a 5% increase in cross-gyre flux compared with that for synthetic drifters with realistic lifetimes. By further advecting synthetic drifters through the observed mean velocity field with and without the Ekman component, estimated from the wind field associated with the actual drifters, it is shown that removal of the Ekman component further increases the intergyre flux by up to 6%. With a turbulent component added to the mean velocity field to simulate the eddy field, there is a further increase in connection by 5%. Thus the Ekman and eddy contributions to the drifter trajectories nearly cancel each other. Consideration of three-dimensional processes (subduction and obduction) is reserved for complete modeling studies.

Citation: Brambilla, E., and L. D. Talley (2006), Surface drifter exchange between the North Atlantic subtropical and subpolar gyres, *J. Geophys. Res.*, *111*, C07026, doi:10.1029/2005JC003146.

1. Introduction

[2] Surface drifters have been extensively used to study the surface circulation in the North Atlantic [*Fratantoni*, 2001; *Flatau et al.*, 2003; *Reverdin et al.*, 2003; *Niiler et al.*, 2003; *McClean et al.*, 2002]. Here, our attention moves beyond the description of Eulerian mean surface currents and we focus on the behavior of surface drifters at the subtropical/subpolar boundary in the North Atlantic, in a manner similar to *Poulain et al.*'s [1996] treatment of Lagrangian drifters in the Norwegian Sea.

[3] We show that there is almost a complete separation between the North Atlantic drifters in the subtropical and subpolar gyres; only one crosses the intergyre boundary. Thus, almost none of the drifters deployed in the subtropical gyre reach the Iceland Basin and the Norwegian Current. Similarly, drifters deployed in the subpolar gyre recirculate cyclonically in the gyre without leaving it.

[4] This observation of so very few surface drifters entering the subpolar gyre contrasts with the known northward upper ocean flow based on surface dynamic topographies [*Reid*, 1994; *Niiler et al.*, 2003] and transport analyses [*Roemmich and Wunsch*, 1985; *Schmitz and McCartney*, 1993; *Macdonald*, 1998; *Koltermann et al.*, 1999; *Ganachaud and Wunsch*, 2003; *Talley et al.*, 2003]. The visual connectivity in the mean surface drifter velocity field from the Gulf Stream through the North Atlantic Current, shown below in section 3, also gives the impression of a northward surface flow from low to high latitudes.

[5] This contrast between the surface drifter trajectories and known net flux based on hydrographic data sets is similar to the situation reported for subsurface floats exiting the Labrador Sea [*Lavender et al.*, 2000]. Although circulation analyses, mass transports and tracers indicate outflow into the Deep Western Boundary Current that heads southwest from Flemish Cap, the floats do not make the connection and instead move eastward, remaining in the subpolar gyre.

[6] On the other hand, it is well-established that jets such as the Gulf Stream have little cross-frontal transport, based on numerous numerical and laboratory models [*Liu and Yang*, 1994; *Yang*, 1996; *Pratt et al.*, 1995; *Berloff et al.*, 2002]. The front that drifters must cross to enter the subpolar gyre is the North Atlantic Current, as or after it turns eastward at the northwest corner [*Rossby*, 1996]. Eddies in these strong currents are a primary mechanism for cross-frontal transport through dispersion [*Bower*, 1991; *Berloff et al.*, 2002; *Ozgokmen et al.*, 2000; *Dutkiewicz et al.*, 1993]. Such an eddy component is of course part of the actual velocity field sampled by the surface drifters; the question is why it is not more effective in creating cross-frontal exchange. A partial answer is suggested by *Owens* [1984], *Bower and Rossby* [1989], *Bower* [1991], and

[1]Scripps Institution of Oceanography, University of California, San Diego, La Jolla, California, USA.

0148-0227/06/2005JC003146$09.00

Lozier and Riser [1990], whose combined observational and modeling studies show that cross-frontal particle exchange is much more inhibited in the strongest frontal flows at the sea surface compared with weaker flows at depth.

[7] Thus the observed dynamic topographies, transport and tracers indicate that there is more rather than less cross-frontal exchange whereas the observed surface drifters suggest that there is less rather than more. How can these two independent and apparently contradictory views of the same circulation be reconciled? We begin by assuming that there must be flow from the subtropical to the subpolar gyre, of up to 20 to 25% of the upper layer of the Gulf Stream, based on meridional transport calculations yielding a 15 to 20 Sv overturn in the northern North Atlantic [*Hall and Bryden*, 1982; *Roemmich and Wunsch*, 1985; *Gordon*, 1986; *McCartney and Talley*, 1982; *Schmitz and McCartney*, 1993; *Richardson and Schmitz*, 1993; *Talley et al.*, 2003; *Lumpkin and Speer*, 2003; *Ganachaud*, 2003]. This provides an upper limit to the intergyre exchange that we might expect.

[8] We then use the surface drifter data observations to begin to evaluate possible mechanisms that could limit the intergyre flux. First, the limited drifter data set and drifter lifetimes might bias the observations. Secondly, the net southward Ekman velocity beneath the westerly winds might counteract the turbulent component of the flow that should cause dispersion of subtropical floats into the subpolar gyre as explored by *Drijfhout et al.* [2003] and *Tansley and Marshall* [2001]. Third, eddies could bias the drifter trajectories since drifters might be trapped in cyclonic eddies and avoid anticyclonic eddies (P. Niiler, personal communication). Fourth, surface water subducts and obducts, particularly in the frontal zone related to the intergyre boundary [*Qiu and Huang*, 1995], but since drifters are constrained to remain at the surface, they cannot follow these three-dimensional pathways.

[9] This paper is limited to investigation of the first two candidates: surface drifter sampling issues and the impact of the Ekman and turbulent components on the drifter trajectories. Analysis of the other possible causes is part of an ongoing study in cooperation with general circulation modelers, in which we are considering the three-dimensionality of the near-surface flow.

[10] The paper is organized as follows: section 2 describes the data and methodology, in section 3 we show the basic drifter observations, focusing on the intergyre boundary, in section 4 the adequacy of the data set and the impact of the Ekman and turbulent components of the flow are analyzed, and section 5 is the summary and conclusions.

2. Data and Methods

[11] Surface drifters drogued at 15m are a large and readily accessible data set, which is expected to be continued indefinitely as part of the global ocean observing system. We examine the subtropical/subpolar northward flow as recorded by this data set in the North Atlantic. As part of our exercise of understanding why the surface drifters do not show cross from the subtropical to the subpolar gyre, we construct a synthetic drifter data set using a simple model based on the surface flow from the actual drifters.

2.1. Observed Drifter Tracks

[12] The Lagrangian surface drifters that are used in this study are part of a large set of drifters deployed in the North Atlantic from 1990 to 2002, under the aegis of the Surface Velocity Program (SVP) established during the WOCE and TOGA experiments, to have a long-term observing system of ocean currents (Figure 1) [*Sybrandy and Niiler*, 1991].

[13] All drifters used in the program were designed with a submerged cylindrical drogue centered at 15 m below the surface, to reduce the slippage due to the wind. The effects of the wind on the drifter trajectory have been estimated by *Niiler* [1995], who showed that the slippage due to the wind for drifters with the drogue attached is limited to 1 cm/s in 10 m/s at 10 m height. *Pazan and Niiler* [2001] compared the response to the wind of drogued and undrogued drifters. The authors concluded that downwind slippage of an undrogued drifter relative to a drogued one is 8.8 cm/s per 10 m/s NCEP wind reanalysis at 10 m height. For a complete description of the SVP drifter refer to *Pazan and Niiler* [2001].

[14] These studies led us to discard undrogued drifters from our data set. After this selection, 1108 drifters were left (98% of the total) to describe the surface circulation in the North Atlantic from 1990 to 2002. Each drifter continuously transmits position (longitude and latitude), temperature and time to the Argos satellite system. The data are processed at the Global Drifter Center at Atlantic Oceanographical and Metereological Laboratory (AOML) which provides them as a time series with a sampling interval of 6 hours. The time series includes: position (longitude and latitude), velocity (zonal and meridional), temperature, time and wind velocity (zonal and meridional). The wind velocity data are obtained by interpolation of the 10 m height NCEP wind reanalysis at 6-hourly intervals at the drifter locations. For a detailed explanation of the data processing, see *Reverdin et al.* [2003].

[15] The mean lifetime of the drogued surface drifters in this data set is 271 days ± 260 days (the median is 182 days). The longest drifter has lifetime of 2024 days, the shortest 1 day.

2.2. Mean Velocity at 15 m

[16] The time series of velocity associated with each drifter has been used to calculate the mean surface velocity field in the North Atlantic. The basin has been divided into a $0.5° \times 0.5°$ grid and the mean vector velocity associated to each grid box is the ensemble average of all the velocity data in the box. The robustness of such binned mean technique has been studied in the past. *Garraffo et al.* [2001b], comparing the true Eulerian mean with binned mean of simulated Lagrangian observation with the MICOM model, showed that in regions characterized by major currents the binned mean overestimates the Eulerian mean, but the difference is not significant with respect to the sampling error. *Lumpkin* [2003] compared the binned mean with the Gauss-Markov (GM) derived mean, demonstrating that both methods agree well in the Atlantic basin, although the Gauss-Markov method shows higher values of the mean velocity in the Gulf Stream.

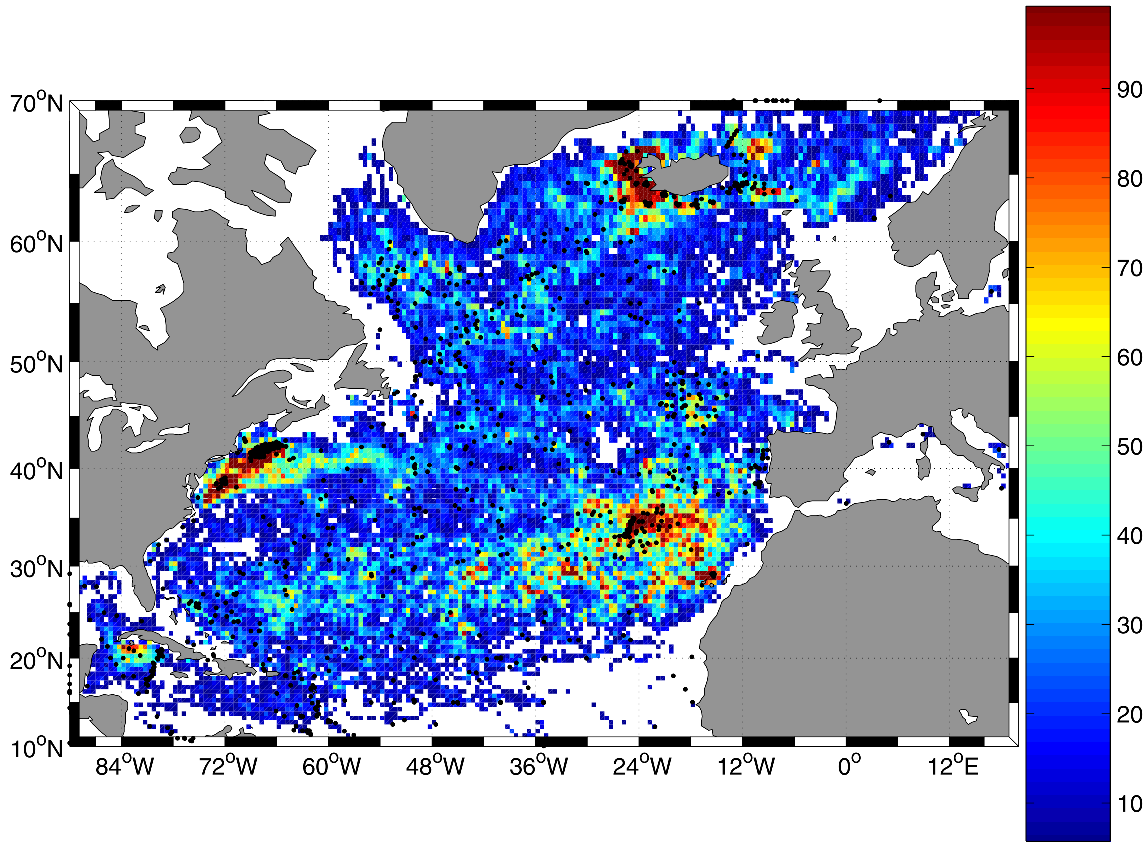

Figure 1. Drifter density (buoy-days) in 0.5° squares. The grid boxes with fewer than 5 buoy-days are not shown. Black dots are drifter deployment locations.

[17] Despite the imprecision of the binned mean in western boundary currents, we consider the estimates of the mean velocity satisfactory, in particular considering that the focus of this study is not a detailed description of the intensity of the currents in the North Atlantic, but rather the tracks of individual drifters.

2.3. Ekman Velocity

[18] The drifter velocity, which is measured at 15 m, can be decomposed into an Ekman component, a geostrophic component, a residual ageostrophic component, and slippage due to the wind.

$$\mathbf{U}(t)_d = \mathbf{U}(t)_e + \mathbf{U}(t)_{geo} + \mathbf{U}(t)_{ageo} + \mathbf{U}(t)_{slip} \tag{1}$$

where $\mathbf{U}(t)_d$ is the velocity measured from the drifter, $\mathbf{U}(t)_e$ is the Ekman component, $\mathbf{U}(t)_{geo}$ is the geostrophic component, $\mathbf{U}(t)_{ageo}$ is the residual ageostrophic component and $\mathbf{U}(t)_{slip}$ is the slippage due to the wind. As mentioned in section 2.1, the slippage velocity due to the wind was quantified by *Niiler* [1995]. The Ekman component is computed using the 6-hourly wind data provided in the drifter data set. After subtracting these from the drifter velocity, the residual velocity includes the geostrophic component, a remaining ageostrophic part and errors related to uncertainties in the Ekman computation and in the wind data.

[19] The Ekman component was calculated for each 6-hourly interval position along each drifter track using the complex-notation formula from *Ralph and Niiler* [1999]:

$$\mathbf{U}_e = \beta e^{-i\theta} u_\circ \frac{\mathbf{t}}{|\tau|} f^{-1/2} \tag{2}$$

In (2), $\mathbf{U}_e = U_e + iV_e$, $\beta = 0.065$, $\theta = 55°$ is the rotation of the Ekman current to the right of the wind, f is the Coriolis parameter, and $u_\circ^2 = \frac{|\tau|}{\rho}$ is the friction velocity, where the wind stress τ is computed using the 10 m NCEP wind reanalysis interpolated at the same 6-hourly interval locations along the drifter tracks. Once the Ralph-Niiler model has been applied, the resulting Ekman velocity is binned and averaged in 0.5° × 0.5° grid boxes to produce the mean Ekman velocity field (Figure 8).

[20] This method of producing an Ekman velocity field in conjunction with drifter data analysis, from the wind data following the drifters and the *Ralph and Niiler* [1999] model, was used by *Flatau et al.* [2003], *Niiler et al.* [2003], and *Lumpkin and Garzoli* [2005] for basin and global-scale analysis of the Ekman and non-Ekman components of the velocity. In contrast, *O'Connor et al.* [2002] used the surface drifters and an estimate of the geostrophic velocity from climatological hydrographic data to construct an Ekman velocity field. As described in *O'Connor et al.* [2002], the comparison between the Ekman velocity field

obtained in this manner agrees with the Ekman velocity expected from the regional wind stress.

2.4. Synthetic Drifters

[21] In order to address the impact on the surface drifter trajectories of possible undersampling, short drifter lifetimes, and the effect of the Ekman and turbulent velocity components, we have created a synthetic drifter data set based on various assumed flow fields constructed from the surface drifter mean field. The trajectories of the synthetic drifters are obtained by advecting artificial particles through the surface velocity field. As opposed to the observed drifters, the synthetic drifters have the advantage of an indefinite lifetime, and the density of the particles can be as large as desired. Furthermore, computing the synthetic drifter trajectories, it is possible to use individual components of the mean velocity field (e.g., total, Ekman and residual) through which the particles are advected to test the impact of each on the trajectories. Noise can also be added to simulate eddies or rms error in the mean velocities.

[22] Two kinds of advection model are used to calculate the trajectory of synthetic drifters. The first is based on simple advection of particles through the mean velocity fields computed from the drifter observations, considering the velocity of the particle at each time step to be completely uncorrelated with the velocity at the immediately previous and following time steps. The second model adds a turbulent component to the mean velocity to simulate eddy noise. The amplitude of the noise is based on the observed standard deviation ellipses from the drifters, to simulate the geographic variation in eddy amplitudes and hence spatial variation in drifter dispersion. The velocity at each time step is set to be partially correlated to the velocity at the previous time step. We refer to the two models as the "mean advection" and "turbulent advection" models.

2.4.1. Mean Advection

[23] The "mean advection" model is

$$\mathbf{r}(t) = \mathbf{u}(t - dt, \mathbf{r}(t - dt))dt + \mathbf{r}(t - dt) \tag{3a}$$

$$\mathbf{u} = \langle \mathbf{U} \rangle_m \tag{3b}$$

alternatively:

$$\mathbf{u} = \langle \mathbf{U} \rangle_m - \langle \mathbf{U} \rangle_e \tag{3c}$$

where $\mathbf{r}(t)$ is the position vector (longitude and latitude); dt is the time step; $\langle \mathbf{U} \rangle_m$ is the mean velocity vector (ensemble average); $\langle \mathbf{U} \rangle_e$ is the mean Ekman component (ensemble average) computed as described in section 2.3.

[24] The mean velocity field and the mean Ekman velocity field are computed on a regular $0.5° \times 0.5°$ grid. A velocity vector is associated with the center of each grid box. At each time step, the mean surface velocity and the mean Ekman velocity that appear in (3b) and (3c) are calculated as the bilinear interpolation, in the location of the particles, of the gridded velocity vectors that surround the position of the particle.

[25] For synthetic drifter runs through the mean field, deployment locations were either: (1) on a regular grid $1° \times 1°$ in a confined region between 78° W–48° W, 35° N–47° N (305 drifters), or (2) at the actual surface drifter release locations (272). A 3-year lifetime was assigned to all synthetic drifters.

2.4.2. Turbulent Advection

[26] The second advection model is based on the advection of artificial particles through the observed mean velocity field with a superimposed turbulence field. The model belongs to the general class of "random flights" models [*Thomson*, 1987]. It simulates the advection of independent particles through a mean velocity field on which is superimposed spatially homogeneous turbulence. This kind of model is commonly used in simulation of Lagrangian advection [e.g., *Dutkiewicz et al.*, 1993; *Falco et al.*, 2000; *Ozgokmen et al.*, 2000; *Castellari et al.*, 2001].

[27] The turbulence is represented by random impulses based on the velocity variance at each grid point computed from the actual surface drifter observations. The model [*Griffa*, 1996] can be written for each component in incremental form as:

$$dx_{1,2} = \left(U_{1,2} + u'_{1,2}\right)dt \tag{4a}$$

$$du'_{1,2} = -\left(\frac{1}{T_L}\right)u'_{1,2}dt + \sqrt{\left(\frac{\sigma^2_{1,2}}{T_L}\right)}dw_{1,2} \tag{4b}$$

where $U_{1,2}$ are the meridional and zonal mean velocity, ${u'}_{1,2}$ are the departure from the mean, $\sigma^2_{1,2}$ is the variance on the ensemble average in each grid box, T_L is the Lagrangian timescale, $dw_{1,2}$ is a random increment from a normal distribution of zero mean and second order - momentum $\langle dw_{1,2}(t_i)\, dw_{1,2}(t_j)\rangle = \delta_{ij}2dt$.

[28] As explained in *Griffa* [1996], (4b) states that at each time step the particle loses a fraction of its momentum, $U(\frac{dt}{T_L})$, and on the other hand receives a random impulse dw. This can also be interpreted as memory of the particle's velocity during a finite time of order T_L.

[29] In the application of the "turbulent advection" model, the time step dt is 6 hours and the total period during which the model runs is 3 years. T_L has been calculated from the drifter data to be 1.5 days for the meridional component and 2.5 days for the zonal component (Appendix A). The deployment locations of the artificial particles follow the same scheme as for the "mean-advection" model (section 2.4.1).

3. Cross Gyre Exchange Observed by Surface Drifters

[30] In this section, we examine the 15-m velocity field given by the surface drifters. We consider the mean flow and individual Lagrangian trajectories. The mean field from surface drifters has been published by multiple authors [*McClean et al.*, 2002; *Flatau et al.*, 2003; *Reverdin et al.*, 2003; *Niiler et al.*, 2003], but the discrepancy between it and the Lagrangian trajectories has not been highlighted.

[31] The surface mean velocity (Figure 2), calculated as described in section 2.2, agrees with the surface mean velocity computed from the same surface drifter data set

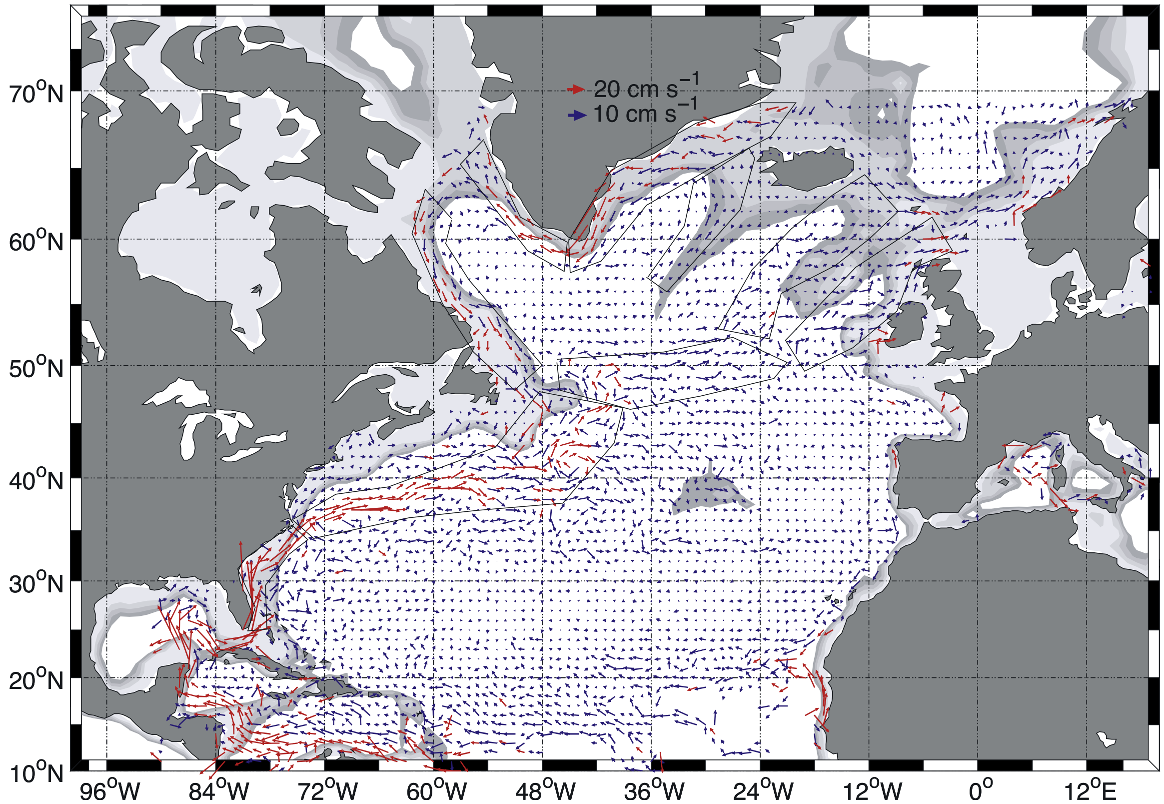

Figure 2. Mean velocity field based on drifter data on a 1° × 1° grid, using a binning technique. The mean has been computed using 15-m drifters with drogues attached. The data cover the period from 1990 to 2002. Red arrows are velocity >20 cm/s. The black boxes identify each current in the North Atlantic. The mean speed of each current is computed averaging the speed inside the boxes. Topography is shaded in gray. The darkest contour is at 2000 m. Contour interval is 500 m.

shown in the cited papers, and captures all the major features of the surface circulation in the North Atlantic.

[32] The strongest currents are the Gulf Stream, along the North American coast, the East and West Greenland Currents, and the Labrador Current along the eastern coast of Canada. Less strong, yet well defined, is the North Atlantic Current (NAC), which, after passing the northwest corner east of the Grand Banks region, crosses the North Atlantic and eventually splits in two branches. One branch passes through the Iceland Basin and the other through Rockall Trough. The mean velocity field also shows a strong Irminger Current, arising on the western flank of the Reykjanes Ridge and connecting to the East Greenland Current.

[33] The mean speed of each surface current listed above has been computed from the drifter velocities and the observed mean surface velocity field (Table 1). For each current, it has been possible to estimate the mean direction of the flow and the standard deviation from the mean. The mean speed for each current, then, is the ensemble average of all the 6-hourly drifter velocities that have direction included in the range provided by the mean direction of the current plus or minus its standard deviation.

[34] Values of mean surface speed from the same Lagrangian drifters have been previously provided by *Fratantoni* [2001]. Our estimates agree in the Gulf Stream, Labrador Current, and East and West Greenland Currents. We use a different division of the NAC (Eastward Branch, Iceland Basin Branch, and Rockall Trough Branch), and we add the Irminger Current mean speed. Our results are also consistent with the mean velocities shown by *McClean et al.* [2002], obtained using just four years (1993–97) of the same data set.

[35] The surface mean velocity field suggests a general tendency of a northward flow from subtropical to subpolar latitudes, through the Gulf Stream and the North Atlantic

Table 1. Speeds of the Strongest Currents in the North Atlantic Based on the Surface Drifter Data[a]

	Mean Speed, cm/s	Max Speed, cm/s
Gulf Stream	66 ± 38	239
Labrador Current	20 ± 12	133
West Greenland Current	21 ± 13	147
East Greenland Current	23 ± 17	185
Irminger Current	6 ± 3	90
NAC (Eastward Branch)	11 ± 7	143
NAC (Iceland Basin Branch)	8 ± 5	82
NAC (Rockall Trough Branch)	10 ± 6	114

[a]Second column is the mean speed (cm/s) and the standard deviation from the mean. The mean speed are computed among the speed of the mean velocity vectors observed inside the black boxes superimposed to the mean velocity field. Just the vectors for which the distribution of the direction of the velocity is approximately Gaussian are considered. Third column is the swiftest drifter observation (cm/s).

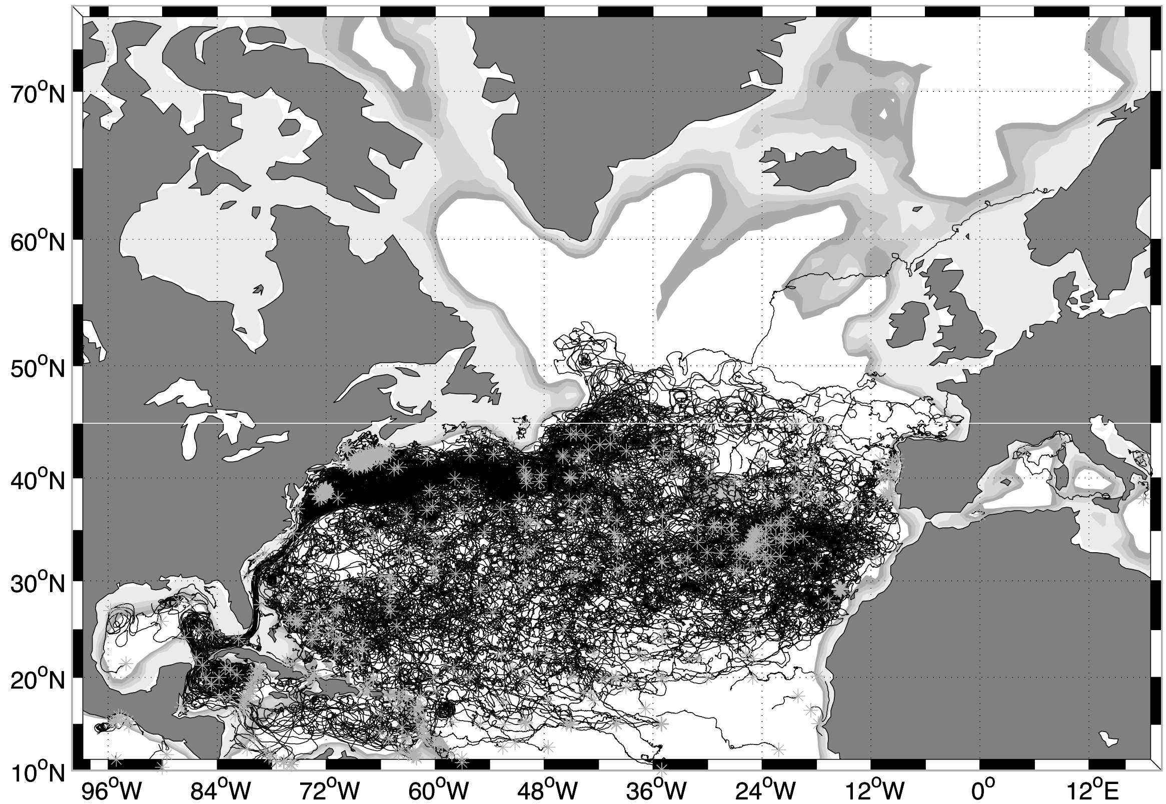

Figure 3. Trajectories of drifters deployed south of 45°N from 1990 to 2002. Gray asterisks are the deployment locations. The white line refers to 45°N. Topography is shaded in gray. The darkest contour is at 2000 m. Contour interval is 500 m.

Current. The Gulf Stream Extension visually appears connected to the North Atlantic Current. As we see next, however, this appearance is misleading.

3.1. Lagrangian Trajectories in the North Atlantic

[36] Based on the appearance of the mean velocity field, one might expect the surface drifters to track the apparent flow that carries water from the subtropical to the subpolar gyre. However, the drifter trajectories do not support this visual interpretation (Figure 3). Of the drifters deployed south of 45°N, only one reached the subpolar gyre.

[37] This drifter had a lifetime of 495 days and had been deployed just south of Newfoundland. Its trajectory followed the edge of the continental shelf, was caught by the permanent Mann eddy east of Newfoundland, and escaped after just 1 loop. It then followed the branch of the NAC that passes through the Rockall Trough, reaching the Norwegian Current. Thus the only connection between the two gyres in the surface drifters is via the northwest corner of the NAC [*Rossby*, 1996]. This location is in agreement with that suggested by the mean velocity field, but the solitary drifter that reached the Norwegian Current cannot represent the expected full intergyre exchange.

[38] For later comparison with synthetic drifter experiments in which we explore the connection of the Gulf Stream extension with the subpolar gyre, we narrow our focus to a rectangular box across the Gulf Stream extension of the following dimensions: 78°W–48°W, 35°N–47°N (hereinafter, Gulf Stream box or GS box) (Figure 4a). 273 drifters flow through this box. Among these, just one reaches the Iceland Basin, which is the same drifter seen in Figure 3.

[39] Drifter deployment within the GS box was not uniform. There was a large concentration of deployments south of Georges Bank, of which about half were lost to the coast while the others were entrained in the Gulf Stream [*Lozier and Gawarkiewicz*, 2001]. This deployment bias could change (reduce) the percentage of GS box drifters that cross to the subpolar gyre, but we would not expect it to reduce the number to just one. Moreover, although the box extends westward including the southward flow of the Middle Atlantic Bight, it is representative of the northward flow since the Middle Atlantic Bight shelf water is eventually entrained in the Gulf Stream [*Churchill and Berger*, 1998]. We explore the issue of deployment bias in section 3.2 using synthetic drifters and conclude that it only affects the precise percentages rather than the general picture, and therefore the use of the box region is a reasonable tool.

[40] On the other hand, of the many drifters that reached the Iceland Basin-Rockall Trough region, most originated in the western part of the subpolar gyre (Labrador and Irminger Seas) (Figure 4b). Again, we cannot conclude that these drifters are tracking water parcels. A simple check of the temperatures recorded by these drifters (with an annual temperature cycle removed) shows a large increase from the Labrador Sea to the northeastern subpolar gyre, which cannot be supported by local air-sea heat fluxes which are neutral or cooling in the annual mean (not shown). Thus we

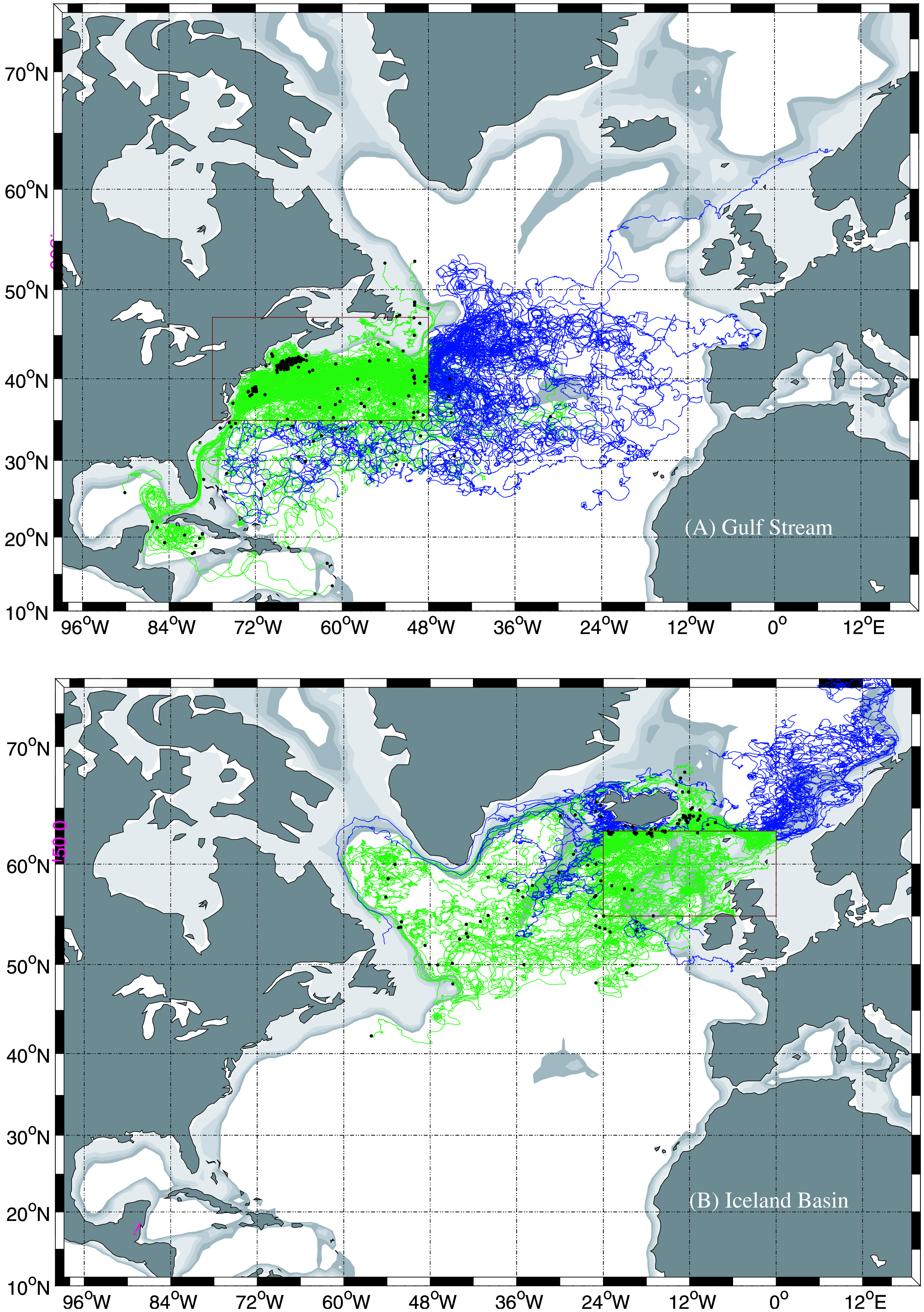

Figure 4. (a) Surface drifter trajectories passing through the Gulf Stream-box (brown). (b) Initial location of surface drifter trajectories passing through the Iceland Basin. Most of the drifters are coming from the west part of the subpolar gyre. For both panels, green trajectories are the drifters before and within the box; blue trajectories are the drifters after exiting the box. Black dots are the deployment locations. Topography is shaded in gray. The darkest contour is at 2000 m. Contour interval is 500 m.

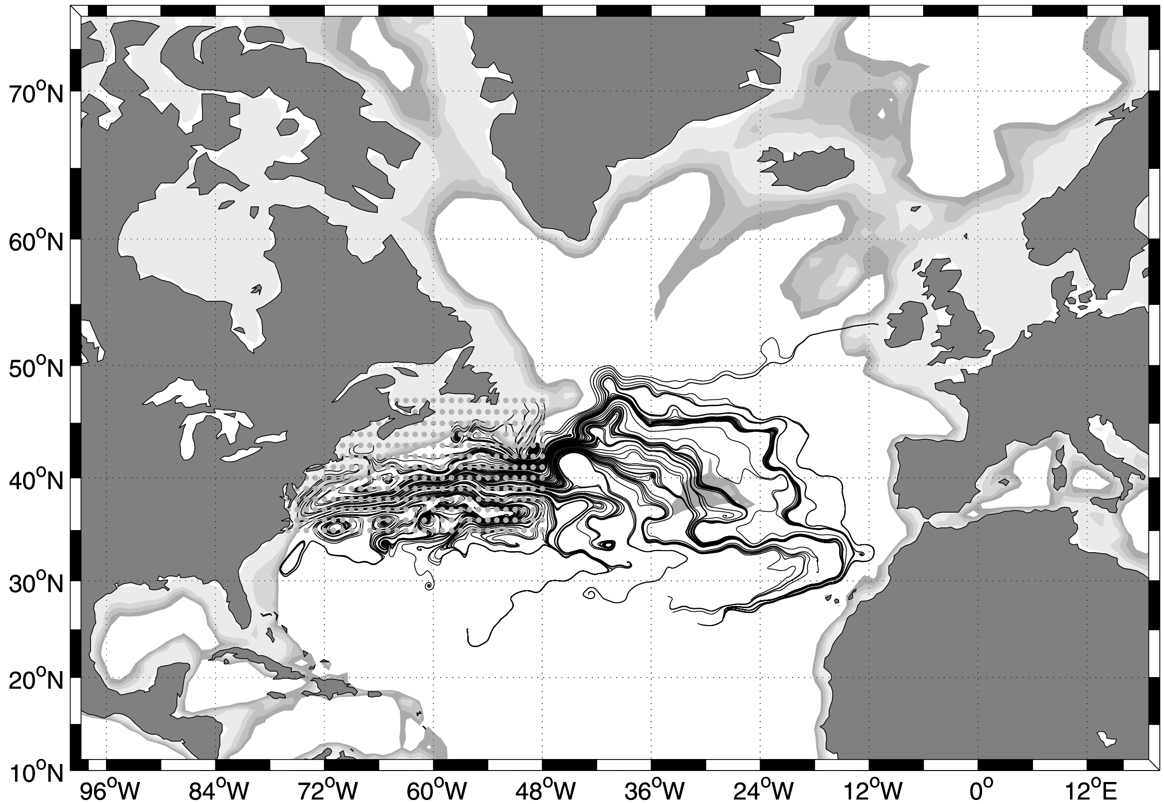

Figure 5. Advection of synthetic drifters through the observed total mean velocity field (Figure 2). This allows an unlimited number of drifters and unlimited drifter lifetime. Total number of synthetic drifters: 305, with a lifetime of 3 years. Drifters entering the subpolar gyre: 3. Gray dots are the deployment locations. Topography is shaded in gray. The darkest contour is at 2000 m. Contour interval is 500 m.

see that drifters constrained to remain at the sea surface clearly cannot represent the three-dimensionality of convecting flow within the Labrador Sea or subducting flow as the currents exit this region of dense surface water.

[41] The nearly complete separation between the gyres in terms of surface drifter trajectories contrasts with the certain connection in the upper ocean between the gyres, from decades of studies of dynamic topographies and meridional transport calculations based on hydrographic data, and with chemical tracers that suggest the connection. As noted in the introduction, the drifter separation is similar to the *Lavender et al.* [2000] result for subsurface floats at 1500 m in the Labrador Sea; floats exiting the Labrador Sea do not continue southward past Flemish Cap to the Deep Western Boundary Current although tracers clearly show the connection.

3.2. Lagrangian Trajectories Using Synthetic Drifters

[42] Our observation of lack of connectivity of surface water from the subtropical to the subpolar gyre could be biased by the limited drifter lifetime of 271 days ± 260 days. Therefore, we conducted experiments with long-lived synthetic particles advected through the observed mean field (section 2.4) to test several potential sources of bias. Although the mean velocity field presented in Figure 2 suggests continuity between the Gulf Stream extension and the North Atlantic Current, artificial particles advected through the same mean do not reproduce the apparent continuity.

[43] Of the 305 synthetic drifters (section 2.4) deployed in the Gulf Stream region on a regular grid with a 3-year lifetime, just 3 enter the subpolar gyre, while the rest remain in the subtropical gyre (Figure 5). When the synthetic drifters are deployed at the release locations of the actual drifters (272 drifters), 15 enter the subpolar gyre. (Results from the synthetic drifters advected through the observed mean velocity field and deployed at the release locations of the observed drifters are highly biased by the spatial inhomogeneity of their initial locations with respect to the coarse grid of the mean velocity field. Drifters deployed at very close locations will be advected by the same vector velocities; therefore the number of Lagrangian trajectories computed in this experiment overestimates the number of independent trajectories.) Table 2 summarizes the number of the actual drifters and synthetic drifters, from the various runs, that enter the subpolar gyre.

[44] We then added turbulent advection proportional to the observed error ellipses to simulate the eddy field (section 2.4.2), and conducted the same two synthetic drifter release experiments. Addition of the eddy field increased the number of synthetic drifters entering the subpolar gyre, to 18 (average) or 6% with a regular grid deployment in the GS box and to 7 (average) or 3% with a deployment at the actual drifter release locations in the GS box. This increase in connectivity was to be expected since eddies increase

Table 2. Summary of the Actual Drifters and All the Synthetic Drifter Runs[a]

Velocity Field	Drifters Released	Drifters in the Subpolar Gyre, %
Actual drifters	273	1 (0.3%)
Observed mean	272 (actual release location)	15 (6%)
Observed mean *without Ekman*	272 (actual release location)	24 (9%)
Observed mean *with turbulence*	272 (actual release location)	7 (3%)
Observed mean *with turbulence and without Ekman*	272 (actual release location)	23 (8%)
Observed mean	305 (regular grid)	3 (1%)
Observed mean *without Ekman*	305 (regular grid)	20 (6%)
Observed mean *with turbulence*	305 (regular grid)	18 (6%)
Observed mean *with turbulence and without Ekman*	305 (regular grid)	36 (12%)

[a]The first column specifies the velocity field through which the artificial particles have been advected. The second column specifies the number of synthetic drifters that have been deployed and the scheme used for their release locations. The third column refers to the number of synthetic drifters and the respective percentage in the subpolar gyre. In all the advection experiments the drifter lifetime is 3 years. The high percentages of the synthetic drifters released in the deployment locations of the actual drifters advected through the observed mean velocity field (second and third row) are biases by the spatial inhomogeneity of their initial locations with respect to the coarse grid of the mean velocity field.

dispersion [*Ozgokmen et al.*, 2000; *Drijfhout et al.*, 2003; *Tansley and Marshall*, 2001], but the resulting gyre connectivity is still not overwhelming.

[45] Thus, caution is necessary to interpret the appearance of the mean velocity field. In fact a northward flow between the two gyres, although indicated by northward transport from low to high latitudes observed using tracers, dynamic topographies and net transport calculations based on hydrography, is reflected in neither the observed nor the synthetic drifter trajectories, with and without eddy noise.

[46] In the next section (4.2), we analyze the disagreement between the appearance of mean velocity field and the Lagrangian trajectories in terms of the Ekman velocity and eddies.

4. Causes for a Low Intergyre Exchange Experienced by Drifters

[47] To investigate possible causes for the low number of drifters that are crossing from the subtropical to the subpolar gyre, we check, first, if the drifter lifetime or the data set density bias the observations. We then examine how the Ekman velocity and eddies affect the drifter trajectories to see if their opposite impact can prevent the drifters from flowing northward. We reserve consideration of the three-dimensionality of the flow for a later study incorporating other data types and general circulation model results.

4.1. Sampling Issues

[48] We first examine the limitation of the drifter data in terms of the number of drifters available (drifter density space) and their lifetime. The average drifter lifetimes are likely shorter than the time necessary to flow from the Gulf Stream region to the subpolar gyre.

4.1.1. Density of the Data Set

[49] The spatial distribution is shown in Figure 1 with density calculated in buoy-days per 0.5° squares; 296,365 total buoy-days are available from the drifters. The spatial distribution of the drifters in the North Atlantic basin is not homogeneous. Three locations have high density: the region just offshore of the west coast of Iceland, the region north of Cape Hatteras, and the region northwest of Africa. Many of the drifters were deployed in these regions, so high concentration is expected and is not related to any specific dynamic process. At 30°N there is another region where there is high drifter concentration, related to convergence in the basin [*Garraffo et al.*, 2001a].

[50] Poorly sampled regions are defined as those with less than 5 buoy-days inside the grid box, thus excluding grid boxes where drifter measurements are completely correlated. *Fratantoni* [2001] applied a similar criterion based on the correlation timescale to select for reliable data in his study, choosing a cutoff Lagrangian timescale of 10 days. However, five days exceeds the highest Lagrangian timescale (3.5 days) calculated for different subregions of the North Atlantic (Appendix A).

[51] The regions of insufficient observations are shelf regions in the Nordic Seas, Labrador Sea, the water offshore Nova Scotia, and along the southeast coast of the U.S.; the shelf regions around France, Ireland, Britain and Norway; and some open ocean regions in the western Sargasso Sea, around 40°N–30°W, and along 50°N. The low drifter density south of 20° N is due to poor sampling, as noted by *Lumpkin and Garzoli* [2005]. Since in this study we are focusing on the subtropical-subpolar flow, these undersampled regions are not a problem.

4.1.2. Observed Drifter Lifetime

[52] The other source of sampling error is drifter lifetime, as already discussed in section 3. The time necessary to flow from the Gulf Stream box to the Iceland Basin is order 400–500 days. This is based on the sole drifter that crossed the intergyre edge and on the average time that other drifters need to cover shorter distances. Drifters with shorter lifetime may not correctly represent the cross-gyre flow.

[53] To estimate the impact of short drifter lifetime on our primary result, the actual drifter trajectories have been combined together into trajectories that last at least 600 days, slightly longer than the 400–500 days mentioned before. To obtain 600-day trajectories, we do the following: (1) remove the seasonal cycle of temperature from each drifter's temperature record; (2) assign a box of fixed dimension (connection area) for each drifter; (3) identify the closest drifter to the center of the connection area and join it to the previous drifter if it satisfies the following temperature criteria.

[54] We do not wish to join trajectories of drifters that are sampling very different water masses. As a crude criterion,

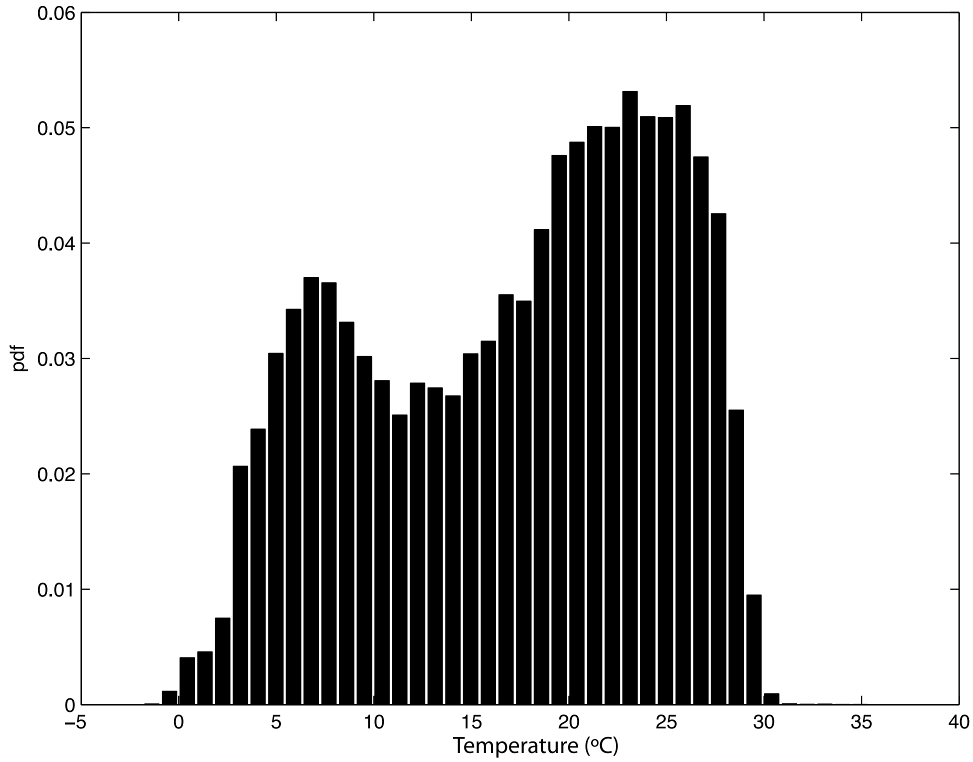

Figure 6. Probability density function of the surface temperature in the North Atlantic basin using drifter temperatures. The peak at lower temperature arises from the subpolar gyre; the peak at higher temperature arises from the subtropical gyre.

we therefore require that the temperatures of the joined drifters not differ greatly from each other. We first remove the seasonal temperature cycle calculated at each geographical location of the drifters using the World Ocean Atlas 1994 (Levitus94). We then join the "original drifter" to the "joining drifter" if:

$$|T_{orig} - T_{join}| < |\Delta T|_{\max} \tag{5}$$

where T_{orig} is the temperature of the "original drifter" at its last known position, and T_{join} is the temperature of the "joining drifter" at the "joining location". $|\Delta T|_{\max}$ is the maximum of the absolute value of temperature difference between the location of the two drifters calculated from the mean temperature field:

$$|\Delta T|_{\max} = |(T_{mean} \pm \sigma)_{orig} - (T_{mean} \pm \sigma)_{join}|_{\max} \tag{6}$$

where $(T_{mean} \pm \sigma)_{orig}$ is the mean temperature at the location of the "original drifter" with its standard deviation, and $(T_{mean} \pm \sigma)_{join}$ is the mean temperature at the location of the "joining drifter" with its standard deviation. The difference of temperature has been calculated from the mean temperature field (without the seasonal cycle) computed with the binning technique ($1^\circ \times 1^\circ$ and $0.5^\circ \times 0.5^\circ$) from the drifter data set. The maximum takes into account the error associated with each mean temperature value.

[55] In addition to this criterion, another constraint is applied in the drifter connection computation. The temperature distribution for the entire North Atlantic is bimodal (Figure 6). The colder peak comes from the subpolar gyre and the warmer from the subtropical gyre.

[56] This suggests that criterion (5) could fail in some regions, since the mean might not be significant. This might be most evident where subtropical and subpolar waters meet, for instance in the region south and east of Newfoundland. To examine the temperature distribution in limited geographical areas, the region between 45° and 55°N has been divided into a regular 1° grid. In the event of bimodal distribution in a given grid box, the temperatures of the two peaks and their standard deviations have been noted. The two modes of the distribution are identified fitting an analytical function to the temperature distribution:

$$f(x)_{fit} = A_1 e^{-\frac{(x-a_1)^2}{2b_1^2}} + A_2 e^{-\frac{(x-a_2)^2}{2b_2^2}} \tag{7}$$

The two maxima and their standard deviations are obtained by the coefficient of the function ($a_{1,2}$, $b_{1,2}$). In case the last known position falls in a box with a bimodal temperature distribution, the following procedure is adopted: first the temperature of the last known position is noted to determine if the drifter comes from a warm or cold water mass. Then, the temperature of the "joining drifter" is required to belong to the same mode of the distribution.

[57] Data sets with 600-day composite trajectories were formed for both 1° and 0.5° squares (size of connection area) (Figure 7). For 1° squares, 60% of the Gulf Stream drifters could be extended to 600-day trajectories. For 0.5° squares, this percentage was 58%. The similarity between

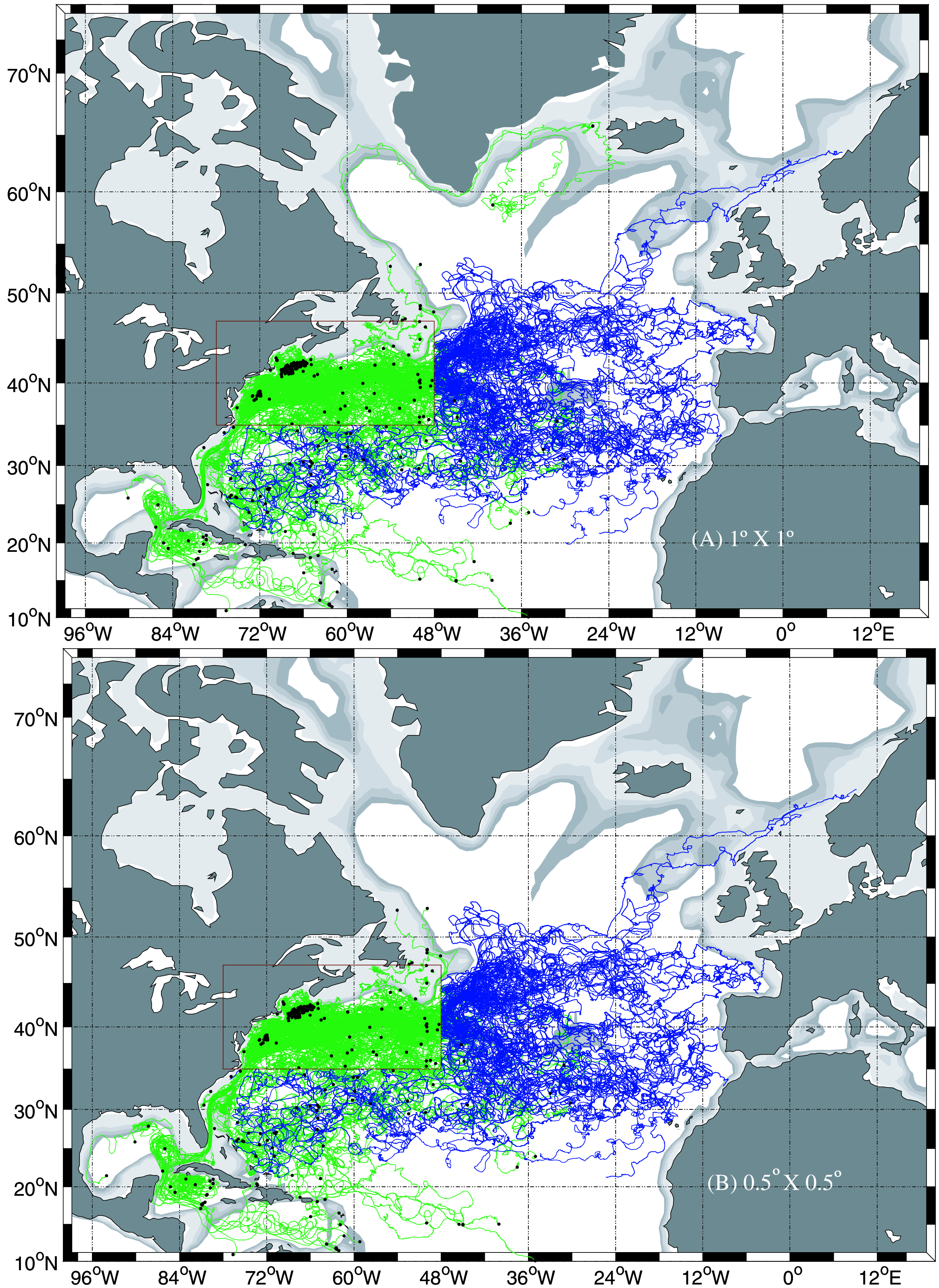

Figure 7. The 600-day combined trajectories (section 4.1.2). Green trajectories are the drifters before and within the Gulf Stream-box; blue trajectories are the drifters after exiting the box. Black dots are the deployment locations. Topography is shaded in gray. The darkest contour is at 2000 m. Contour interval is 500 m. (a) Using a connection area of $1^\circ \times 1^\circ$; 5% of the connected trajectories cross into the subpolar gyre. (b) Using a connection area of $0.5^\circ \times 0.5^\circ$; 4% enter the subpolar gyre.

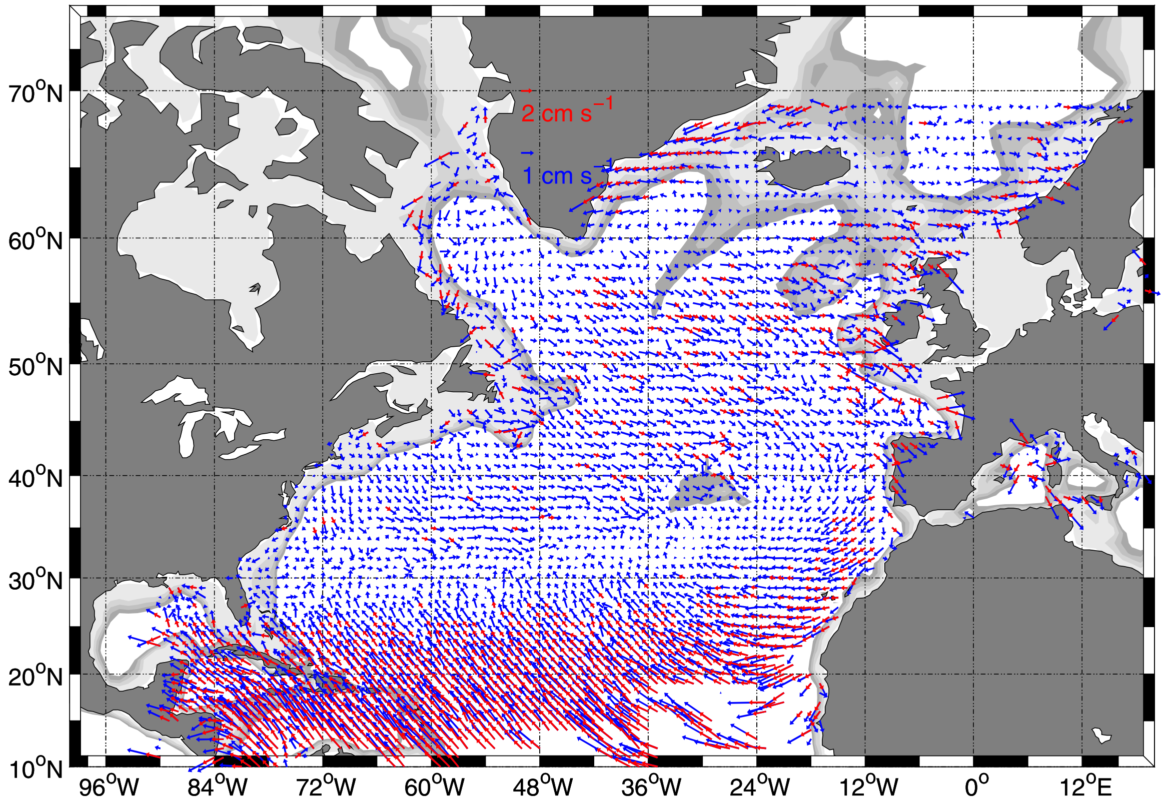

Figure 8. Mean Ekman velocity field in 1° × 1° calculated from wind data. Red arrows are velocity >2 cm/s. Topography is shaded in gray. The darkest contour is at 2000 m. Contour interval is 500 m.

the percentage of 600-day trajectories with different size of connection area suggests that reduction to the 0.5° grid still provides adequate data density. For 1° (0.5°) squares, 15% (20%) could not be joined because there were no drifters passing through the connection area, while 20% (19%) could not be joined because of the temperature requirement. The other connection failure is due to drifters that exit the study domain.

[58] With extended drifter trajectories joined in 0.5° squares the percentage of drifters that flow from the Gulf Stream-box to the subpolar gyre increases to 4%. With 1° squares, 5% enter the subpolar gyre. This suggests that the solitary actual drifter that crossed the intergyre edge underestimates the total number of drifters that would be carried by the Gulf Stream to the subpolar gyre given much longer drifter lifetimes.

4.1.3. Synthetic Drifter Lifetime

[59] Synthetic drifter trajectories can also provide information on the importance of lifetime in biasing the observations of cross-gyre connections. In section 3.2, synthetic tracks were computed using the observed mean velocity field and a "mean-advection" model (section 2.4.1). Synthetic drifters calculated with the "mean-advection" model have been set to last 3 years (1095 days), which should be sufficient for cross-gyre flow. Despite the long lifetime, the number of drifters flowing into the subpolar gyre (Figure 5) is very low: only 3 synthetic drifters cross the intergyre edge.

[60] The low number of synthetic drifters in the subpolar gyre, despite the long lifetime, is confirmed by synthetic drifters advected through the mean velocity field with a turbulent component added to it (section 2.4.2). When the synthetic drifters are released on a regular grid, an average of 18 (5%) reach the subpolar gyre. When the synthetic drifters are deployed at the release locations of the actual drifters, an average of 7 drifters (3%) flow north into the subpolar gyre. This confirms the result obtained in section 4.1.2. Hence, drifter lifetime biases the observations, underestimating the Lagrangian trajectories that cross the intergyre boundary.

4.2. Ekman Velocity Bias and Effects of Eddies

[61] The Ekman velocity is another possible source of bias for the representation of the cross-gyre flow by surface drifters. Figure 8 shows the mean Ekman velocity field in the North Atlantic from the winds observed simultaneously with the surface drifter observations, then using the Ralph-Niiler model (section 2.1). The computation presented here agrees with the mean Ekman velocity field described in *Flatau et al.* [2003]. The average Ekman speed is order 1 cm/s, as reported in *Flatau et al.* [2003]. Although Ekman is a small fraction of the total velocity of the drifters, it could still significantly affect the drifter trajectories, acting as a southward forcing that prevents the drifters from crossing to the north.

[62] To address the effect of the Ekman component and eddies, we use synthetic drifters (section 2.4) propagated through various components of the same observed mean velocity field. The Ekman component and the turbulent component are removed or added to the observed mean

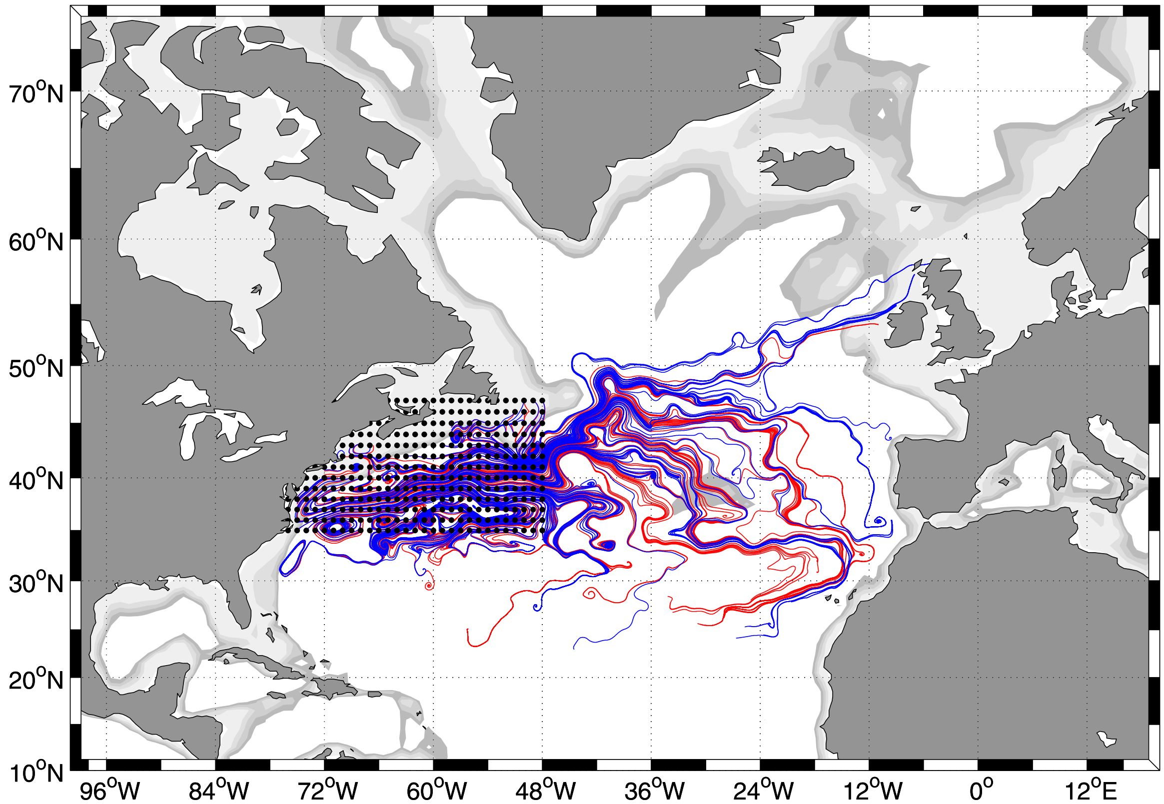

Figure 9. Advection of synthetic drifters through the observed mean velocity field. Red: trajectories advected through the total mean velocity field (already shown in Figure 5). Drifters entering the subpolar gyre = 3. Blue: trajectories advected through the mean velocity field without the Ekman component. Drifters entering the subpolar gyre = 20. In both cases (red and blue) the total number of synthetic drifters is 305, with a lifetime of 3 years. Black dots are the synthetic drifter deployment locations. Topography is shaded in gray. The darkest contour is at 2000 m. Contour interval is 500 m.

velocity field to obtain four different sets of synthetic drifters that are, then, compared.

[63] Synthetic drifters advected through the simple observed mean velocity field were introduced in section 3.1 to highlight the visually misleading continuity between the subtropical and subpolar gyres and to consider the influence of limited drifter lifetime on the gyre connection.

[64] Here, we compare synthetic trajectories advected through the mean velocity field in which the Ekman component is retained and synthetic trajectories computed through the same mean field from which the Ekman component has been removed (Figure 9). As shown previously (section 3.2), only 3 synthetic drifters (1% of 305) cross into the subpolar gyre when we use the total mean which includes the Ekman component. When Ekman is removed, more drifters move north in the North Atlantic Current with 20 (6%) reaching the subpolar gyre.

4.3. Advection Experiment Including Turbulence

[65] The actual oceanic velocity field includes an eddy field, which can be thought of as random turbulence added to the mean. Cross-gyre transport should be augmented by turbulence [*Bower*, 1991; *Berloff et al.*, 2002], which is normally associated with dispersion about the mean.

[66] As already described (section 2.4.2), the turbulence is parameterized by a random value added at each time step based on the velocity variance at each grid box. Since the addition of a random impulse makes each model run unique, the numerical experiments have been repeated several times. We ran the "turbulent-advection" model 9 times retaining the Ekman component (Figure 10a), and 9 times removing Ekman (Figure 10b). The reported fraction of drifters that enter the subpolar gyre is the average of the runs.

[67] The results are that 6% of the synthetic drifters in the "turbulent-advection" model with the total mean velocity reach the Iceland Basin-Rockall Trough region. When the Ekman component is removed, 12% of synthetic drifters flow northward.

[68] These results lead to two separate conclusions. The synthetic drifter runs, with and without turbulence, show that removal of Ekman velocity increases by up to 5–6% the number of drifters crossing to the subpolar gyre. Likewise and separately, addition of a turbulent component, with and without Ekman, increases by up to 5–6% the number of drifters reaching the subpolar gyre.

[69] Thus the Ekman velocity and eddies counteract each other in this region, in agreement with the model study by *Drijfhout et al.* [2003]. The opposite impact of the two processes is of course not dynamical, but is an artifact of the location of the study area in a region of southward Ekman transport. Eddy noise itself always increases dispersion, and

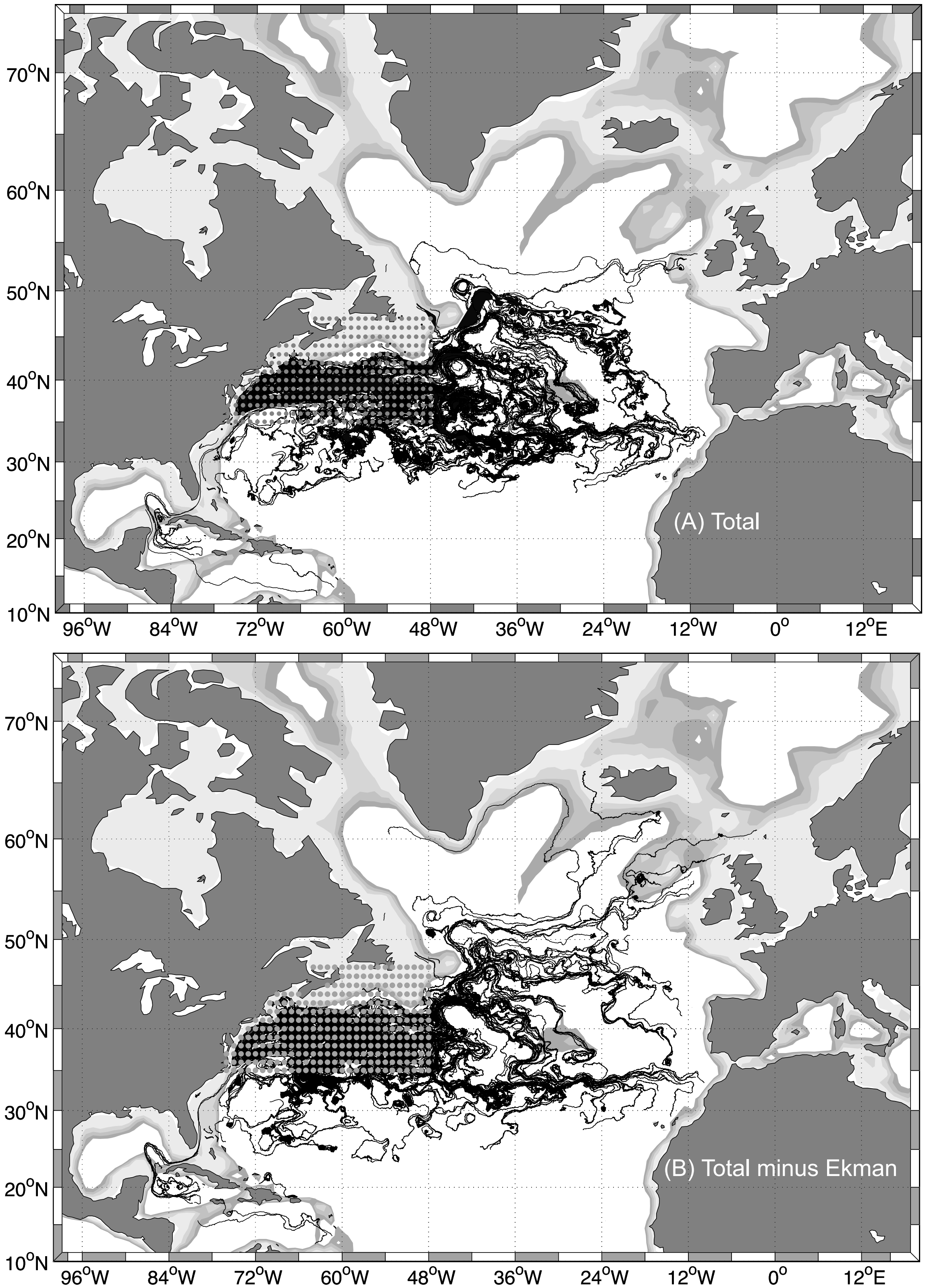

Figure 10. Synthetic drifters advected through the mean velocity field with random turbulence added to it. In both cases the number of synthetic drifters is 305 with a lifetime of 3 years. Gray dots are the deployment locations. Topography is shaded in gray. The darkest contour is at 2000 m. Contour interval is 500 m. (a) Synthetic drifters advected through the total mean with random turbulence. Average of drifters entering the subpolar gyre:18. (b) Synthetic drifters advected through the mean velocity field after removing the Ekman component. Random turbulence is added to the mean. Average of drifters entering the subpolar gyre: 36.

therefore results in increased leakage to the subpolar gyre of drifters released in the subtropical gyre. It is though notable that in our study as well as in *Drijfhout et al.* [2003], the two effects are of the same order of magnitude.

5. Summary and Conclusion

[70] In this paper we described the surface drifter exchange between the subtropical and subpolar gyres in the North Atlantic. Surface drifters deployed in the subtropical gyre mostly recirculate within the gyre. Just one drifter in this twelve-year data set crossed from the subtropical gyre northward into the subpolar gyre, which was surprising given the known connectivity between the gyres based on many decades of hydrographic and tracer analyses.

[71] The steps that we have taken to understand the observed separation between subtropical and subpolar drifters led us to the following conclusions. (1) Limited drifter lifetime results in an underestimate of the northward flux, based on constructing 600-day trajectories from the actual drifter data. With the extended trajectories the number of drifters from the GS area to the subpolar gyre increases from 1% to 5%. (Drifter density was judged to be sufficient based on the Lagrangian timescale of the drifters presented in Appendix A and in a number of previous works.) (2) The mean flow observed by the surface drifters, which includes the Ekman component, does not produce synthetic drifter trajectories that cross from the subtropical to the subpolar gyre, even with long synthetic drifter lifetimes. (3) The Ekman component of the flow counteracts the turbulent component, preventing the drifters from crossing the intergyre edge. Using a basic advection model, the percentage of synthetic drifters flowing from the subtropical to the subpolar gyre increases by up 5–6% when the Ekman component is removed from the mean velocity field. On the other hand, the number of synthetic drifters in the subpolar gyre advected through the observed mean velocity field to which a turbulent component has been added increases by up 5–6%.

[72] We conclude that sampling bias and Ekman velocity contribute to the drifter separation between the subtropical and subpolar gyre in the North Atlantic, while turbulent eddies act to increase the connectivity. The Ekman and turbulent contributions are of the same order of magnitude. Therefore, if one had Lagrangian drifters in the upper ocean but below the Ekman layer, one might expect somewhat more connectivity, on the order of 5–6% of the drifters. This is still well below the 20% or so of the upper Gulf Stream that should move to the subpolar gyre as part of the meridional overturning circulation. We are in the process of exploring the role of the three dimensionality of the flow using particle tracing in general circulation models; this is expected to yield the rest of the connecting flow.

Appendix A: Lagrangian Timescale

[73] The computation of the Lagrangian timescale follows the procedure described in many previous studies [*Garraffo et al.*, 2001a; *Zhang et al.*, 2001; *McClean et al.*, 2002; *Lumpkin et al.*, 2002]. The Lagrangian timescale in the North Atlantic from surface drifters represents the interval in time in which the velocity of the drifters are strongly correlated. In order to calculate it from the 15-m drogued drifters, we divided each drifter track in segments of 50 days, to exclude any correlation of drifter velocity over a time longer than 50 days. For each segment the autocorrelation function has been calculated

$$C_{1,2}(\tau) = \frac{1}{\sigma_{1,2}^2} R_{1,2}(\tau) \quad \text{(A1)}$$

where $\sigma_{1,2}^2$ is the variance and $R_{1,2}$ is the Lagrangian temporal autocovariance function, computed for each component as:

$$R_{1,2}(\tau) = \langle \left(u_{1,2}(t) - \overline{u_{1,2}}(t)\right)\left(u_{1,2}(t+\tau) - \overline{u_{1,2}}(t)\right)\rangle \quad \text{(A2)}$$

where $\langle\ \rangle$ indicates expected values, $\overline{u}$ is the mean velocity component in the drifter segment and τ is the time lag. The indices 1,2 refer to the meridional and zonal components. After calculating the average of the autocorrelation function from the segments, the Lagrangian timescale is:

$$T_{L1,2} = \int_0^{\infty} C_{1,2}(\tau) d\tau \quad \text{(A3)}$$

where $C(\tau)$ is the autocorrelation function. Due to the impossibility of extending the integral in (A3) to ∞, following the general practice suggested by other calculations [*Böning*, 1988], (A3) is simplified to:

$$T_{L1,2} = \int_0^{\tau_0} C_{1,2}(\tau) d\tau \quad \text{(A4)}$$

where τ_0 is the first zero crossing of the autocorrelation function. The choice of the first zero crossing is also justified by the fact that the autocorrelation function tends to be dominated by noise for large lags [*Lumpkin et al.*, 2002].

[74] Although the Lagrangian timescale from surface drifters has been calculated in different subregions of the North Atlantic, the value T_L that has been used to calculate the trajectory of the synthetic drifters is constant in space and corresponds to the T_L in the Gulf Stream and North Atlantic Current region. For the meridional component we found T_L = 1.5 days; for the zonal component we found T_L = 2.5. These are consistent with the previous studies here cited.

[75] **Acknowledgments.** This study was supported by the National Science Foundation Ocean Sciences Division through grants OCE-9529584 as part of the World Ocean Circulation Experiment and OCE-0424893 as part of the CLIVAR CLIMODE experiment. We thank Peter Niiler for supplying the drifter and wind data.

References

Berloff, P., J. C. McWilliams, and A. Bracco (2002), Material transport in oceanic gyres. Part I: Phenomenology, *J. Phys. Oceanogr.*, *32*(3), 764–796.

Böning, C. (1988), Characteristics of particle dispersion in the North Atlantic: An alternative interpretation of SOFAR float results, *Deep Sea Res.*, *35*, 1379–1385.

Bower, A. S. (1991), A simple kinematic mechanics for mixing fluid particles across a meandering jet, *J. Phys. Oceanogr.*, *21*, 173–180.

Bower, A. S., and H. T. Rossby (1989), Evidence of cross-frontal exchange processes in the gulf stream based on isopycnal rafos float data, *J. Phys. Oceanogr.*, *19*, 1177–1190.

Castellari, S., A. Griffa, T. M. Ozgokmen, and P.-M. Poulain (2001), Prediction of particle trajectories in the Adriatic Sea using Lagrangian data assimilation, *J. Mar. Syst.*, *29*, 33–57.
Churchill, J., and T. Berger (1998), Transport of Middle Atlantic Bight shelf water to the Gulf Stream near Cape Hatteras, *J. Geophys. Res.*, *103*(C13), 30,605–30,621.
Drijfhout, S. S., P. de Vries, K. Döös, and A. C. Coward (2003), Impact of eddy-induced transport on the Lagrangian structure of the upper branch of the thermohaline circulation, *J. Phys. Oceanogr.*, *33*, 2141–2155.
Dutkiewicz, S., A. Griffa, and D. B. Olson (1993), Particle diffusion in a meandering jet, *J. Geophys. Res.*, *98*, 16,487–16,500.
Falco, P., A. Griffa, A. Poulain, P.-M. Poulain, and E. Zambianchi (2000), Transport properties in the Adriatic Sea deduced from drifter data, *J. Phys. Oceanogr.*, *30*, 2055–2071.
Flatau, M. K., L. D. Talley, and P. P. Niiler (2003), The North Atlantic Oscillation, surface current velocities and SST changes in the subpolar North Atlantic, *J. Clim.*, *16*, 2355–2369.
Fratantoni, D. M. (2001), North Atlantic surface circulation during the 1990s observed with satellite-tracked drifters, *J. Geophys. Res.*, *106*(C10), 22,067–22,093.
Ganachaud, A. (2003), Large-scale mass transports, water mass formation, and diffusivities estimated from World Ocean Circulation Experiment (WOCE) hydrographic data, *J. Geophys. Res.*, *108*(C7), 3213, doi:10.1029/2002JC001565.
Ganachaud, A., and C. Wunsch (2003), Large-scale ocean heat and freshwater transports during the World Ocean Circulation Experiment, *Clim, J.*, *16*, 696–705.
Garraffo, Z. D., A. J. Mariano, A. Griffa, C. Veneziani, and E. P. Chasignet (2001a), Lagrangian data in a high-resolution numerical simulation of the North Atlantic I. Comparison with in situ drifter data, *J. Mar. Syst.*, *29*, 157–176.
Garraffo, Z. D., A. J. Mariano, A. Griffa, C. Veneziani, and E. P. Chasignet (2001b), Lagrangian data in a high-resolution numerical simulation of the North Atlantic II. On the pseudo-Eulerian averaging of Lagrangian data, *J. Mar. Syst.*, *29*, 177–200.
Gordon, A. L. (1986), Interocean exchange of thermocline water, *J. Geophys. Res.*, *91*, 5037–5046.
Griffa, A. (1996), Applications of stochastic particle models to oceanographic problems, in *Stochastic Modelling in Physical Oceanography*, vol. 24, edited by R. Adler, P. Muller, and B. Rozovskii, 467 pp., Springer, New York.
Hall, M., and H. Bryden (1982), Direct estimates and mechanism of ocean heat transport, *Deep Sea Res.*, *29*, 339–359.
Koltermann, K. P., A. V. Sokov, V. P. Tereschenkov, S. A. Dobroliubov, K. Lorbacher, and A. Sy (1999), Decadal changes in the thermohaline circulation of the North Atlantic, *Deep Sea Res.*, *46*, 109–138.
Lavender, K. L., R. E. Davis, and W. B. Owens (2000), Mid-depth recirculation observed in the interior Labrador and Irminger seas by direct velocity measurements, *Nature*, *407*, 66–69.
Liu, Z., and H. Yang (1994), The intergyre chaotic transport, *J. Phys. Oceanogr.*, *24*, 1768–1782.
Lozier, M. S., and G. Gawarkiewicz (2001), Cross-frontal exchange in the Middle Atlantic Bight as evidenced by surface drifters, *J. Phys. Oceanogr.*, *31*, 2498–2510.
Lozier, M. S., and S. C. Riser (1990), Potential vorticity sources and sinks in a quasi-geostrophic ocean: Beyond western boundary currents, *J. Phys. Oceanogr.*, *20*, 1608–1627.
Lumpkin, R. (2003), Decomposition of surface drifter observations in the Atlantic Ocean, *Geophys. Res. Lett.*, *30*(14), 1753, doi:10.1029/2003GL017519.
Lumpkin, R., and S. Garzoli (2005), Near surface circulation in the Tropical Atlantic Ocean, *Deep Sea Res., Part I*, *52*, 495–518.
Lumpkin, R., and K. Speer (2003), Large-scale vertical and horizontal circulation in the North Atlantic Ocean, *J. Phys. Oceanogr.*, *33*, 1902–1920.
Lumpkin, R., A. Treguier, and K. Speer (2002), Lagrangian eddy scales in the North Atlantic Ocean, *J. Phys. Oceanogr.*, *32*, 2425–2440.
Macdonald, A. (1998), The global ocean circulation: A hydrographic estimate and regional analysis, *Prog. Oceanogr.*, *41*, 281–382.
McCartney, M., and L. D. Talley (1982), The subpolar mode water of the North Atlantic, *J. Phys. Oceanogr.*, *12*, 1169–1188.
McClean, J. L., P.-M. Poulain, J. W. Pelton, and M. E. Maltrud (2002), Eulerian and Lagrangian statistics from surface drifters and a high-resolution POP simulation in the North Atlantic, *J. Phys. Oceanogr.*, *32*, 2472–2491.
Niiler, P. P. (1995), Measurements of the water-following capability of holey-sock and TRISTAR drifters, *Deep Sea Res., Part I*, *42*, 1951–1964.
Niiler, P. P., N. A. Maximenko, and J. C. McWilliams (2003), Dynamically balanced absolute sea level of the global ocean derived from near-surface velocity observations, *Geophys. Res. Lett.*, *30*(22), 2164, doi:10.1029/2003GL018628.
O'Connor, B. M., R. A. Fine, K. A. Maillet, and D. B. Olson (2002), Formation rates of subtropical underwater in the Pacific Ocean, *Deep Sea Res., Part I*, *49*, 1571–1590.
Owens, W. B. (1984), A synoptic and statistical description of the Gulf Stream and subtropical gyre using SOFAR floats, *J. Phys. Oceanogr.*, *14*, 104–113.
Ozgokmen, T. M., A. Griffa, A. J. Mariano, and L. I. Piterbarg (2000), On the predictability of Lagrangian trajectories in the ocean, *J. Atmos. Oceanic Technol.*, *17*, 366–383.
Pazan, S. E., and P. P. Niiler (2001), Recovery of near-surface velocity from undrogued drifters, *J. Atmos. Technol.*, *18*, 476–489.
Poulain, P., A. Warn-Varnas, and P. Niiler (1996), Near-surface circulation of the Nordic seas as measured by Lagrangian drifters, *J. Geophys. Res.*, *101*, 18,237–18,258.
Pratt, J., M. Lozier, and N. Beliakova (1995), Parcel trajectories in quasi-geostrophic jets: Neutral models, *J. Phys. Oceanogr.*, *22*, 431–440.
Qiu, B., and R. X. Huang (1995), Ventilation of the North Atlantic and North Pacific: Subduction versus Obduction, *J. Phys. Oceanogr.*, *8*, 2374–2390.
Ralph, E., and P. Niiler (1999), Wind-driven currents in the tropical Pacific, *J. Phys. Oceanogr.*, *29*, 2121–2129.
Reid, J. (1994), On the total geostrophic circulation of the North Atlantic Ocean: Flow patterns, tracers and transports, *Prog. Oceanogr.*, *33*, 1–92.
Reverdin, G., P. P. Niiler, and H. Valdimarsson (2003), North Atlantic Ocean surface currents, *J. Geophys. Res.*, *108*(C1), 3002, doi:10.1029/2001JC001020.
Richardson, P., and W. J. Schmitz (1993), Deep cross-equatorial flow in the Atlantic measured with SOFAR floats, *J. Geophys. Res.*, *98*(C5), 8371–8387.
Roemmich, D., and C. Wunsch (1985), Two translatantic sections: Meridional circulation and heat flux in the subtropical North Atlantic Ocean, *Deep Sea Res.*, *32*, 619–664.
Rossby, T. (1996), The North Atlantic current and surrounding waters: At the crossroads, *Rev. Geophys.*, *34*, 463–481.
Schmitz, W. J., and M. S. McCartney (1993), On the North Atlantic circulation, *Rev. Geophys.*, *31*, 29–49.
Sybrandy, A. L., and P. P. Niiler (1991), WOCE/TOGA Lagrangian drifter constructin manual, *SIO Ref. 9/16, WOCE Rep. 63*, 58 pp.
Talley, L., J. L. Reid, and P. E. Robbins (2003), Data-based meridional overturning streamfunctions for the global ocean, *J. Clim.*, *16*, 3213–3226.
Tansley, C. E., and D. P. Marshall (2001), On the dynamics of wind-driven circumpolar currents, *J. Phys. Oceanogr.*, *31*, 3258–3273.
Thomson, D. J. (1987), Criteria for the selection of stochastic models of particle trajectories in turbulent flows, *J. Fluid Mech.*, *180*, 529–556.
Yang, H. (1996), The subtropical/subpolar gyre exchange in the presence of annually migrating wind and a meandering jet: Water mass exchange, *J. Phys. Oceanogr.*, *26*, 115–130.
Zhang, H. M., M. D. Prater, and T. Rossby (2001), Isopycnal Lagrangian statistics from the North Atlantic Current RAFOS float observations, *J. Geophys. Res.*, *106*, 13,817–13,836.

E. Brambilla and L. D. Talley, Scripps Institution of Oceanography, University of California, San Diego, 9500 Gilman Dr., La Jolla, CA 92093-0208, USA. (ebrambilla@ucsd.edu)